Large Group Delay in Silicon-on-Insulator Chirped Spiral Bragg Grating Waveguide

Yu Sun, Dongyu Wang, Chunyu Deng, Mengjia Lu, Lei Huang, Guohua Hu, Binfeng Yun, Ruohu Zhang, Ming Li, Jianji Dong, Anle Wang, and Yiping Cui

***Abstract*—Limited by large transmission loss, the development of transverse electric (TE) mode silicon-on-insulator (SOI) based on-chip long length chirped grating waveguide faces many difficulties now. To overcome this problem, multi-mode waveguide with a measured transmission loss of 0.7 dB/cm is applied in this paper, and a chirped spiral Bragg grating waveguide (SBGW) is proposed and experimentally demonstrated. The length of the chirped SBGW reaches 2.7 cm, which is the longest SOI based grating reported so far. The total group delay is measured to be 628 ps, with a structure size of only 0.3 mm^2 due to the application of spiral configuration. The slope of the linear dispersion is -27.7 ps/nm. This integrated chirped SBGW shows great compatibility with frequently used TE mode SOI devices and has great potential for applications in microwave photonics requiring dispersion control.**

***Index Terms*—Spiral Bragg grating waveguide, linear dispersion, group delay, integrated optics.**

I. Introduction

BRAGG gratings have developed extensive applications in optical devices for communication [1]–[3], sensing [4], [5], signal processing [6]–[9], etc. In recent years, the development of integrated on-chip Bragg gratings has become an inevitable trend, and tremendous amount of researches on waveguide Bragg gratings has emerged [10]–[12]. Nowadays, the requirement for long length Bragg gratings with chirp has become increasingly urgent in fields such as dispersion compensation [13], [14] and frequency-time mapping [15]–[18]. When it comes to long length gratings, a spiral configuration shows better process consistency and compactness [19], [20], comparing to straight grating waveguide. Until now, most integrated Bragg gratings based on silicon-on-insulator (SOI) platform are designed for transverse electric (TE) single-mode operation [21]–[24]. However, due to the large propagation loss, TE single-mode grating waveguide cannot be a solution to long length integrated Bragg grating. To reduce the propagation loss, chirped spiral Bragg grating waveguides (SBGW) operating in transverse magnetic (TM) modes are proposed and characterized [25], [26], while extra complexity will be introduced when integrating such SBGW with commonly used TE mode elements. Another practical approach to realizing long length integrated Bragg grating on SOI platform is the large cross section rib waveguide [27]. The propagation loss can be relatively low. However, the minimum bending radius is much larger than the 220 nm thick stripe waveguide, which is disadvantageous to compact integration, and the non-standard top silicon thickness will increase the fabrication complexity. Moreover, comparing to other low loss platforms such as silicon nitride and silicon dioxide, SOI based design has obvious advantages in compact integration and active tuning.

In this paper, to realize a total group delay of more than 500 ps, a chirped spiral Bragg grating based on TE mode waveguide fabricated on SOI platform is demonstrated. 1200 nm wide multi-mode waveguide is applied to reduce the transmission loss for the realization of large time delay on standard 220 nm top silicon. Parameters such as bending radius and waveguide gap are analyzed and optimized, and the impacts on bandwidth and group delay ripples after apodization are also studied in our work. A TE mode chirped SBGW on conventional 220 nm SOI platform with large time delay, low transmission loss and low ripples is successfully developed.

II. Design and Simulation

In our design, the chirped grating waveguide is wrapped into two Archimedean spirals and an S-shaped waveguide consisting of two semi-circular waveguides. Fig. 1(a) is the schematic of the chirped SBGW. An average waveguide width of 1200 nm is selected since it has no more than 3 TE modes, and its propagation loss and sensitivity to sidewall roughness are dramatically reduced comparing with a single TE mode waveguide [28]. To maintain low propagation loss, extra loss caused by a too small bending radius must be avoided. To determine the minimum

Manuscript received September 5, 2021; accepted September 11, 2021. Date of publication September 16, 2021; date of current version October 1, 2021. *(Corresponding author: Guohua Hu.)*

Yu Sun, Chunyu Deng, Mengjia Lu, Guohua Hu, and Binfeng Yun are with the Advanced Photonics Center, Southeast University - Sipailou Campus, Nanjing 210096, China (e-mail: 230189799@seu.edu.cn; dcy@seu.edu.cn; mjlu@seu.edu.cn; photonics@seu.edu.cn; ybf@seu.edu.cn).

Dongyu Wang and Ruohu Zhang are with the School of Electronic Science and Engineering, Southeast University, Nanjing 210096, China (e-mail: 230208131@seu.edu.cn; zrh@seu.edu.cn).

Lei Huang is with the Southeast University - Sipailou Campus, Nanjing 210096, China (e-mail: 230189110@seu.edu.cn).

Ming Li is with the Institute of Semiconductor, Chinese Academy of Sciences, Beijing 100086, China (e-mail: ml@semi.ac.cn).

Jianji Dong is with the School of Optoelectronic Science and Engineering, Wuhan National Lab for Optoelectronics, Wuhan 430074, China (e-mail: jjdong@mail.hust.edu.cn).

Anle Wang is with the Microwave Photonics Research Center, People's Liberation Army Air Force Early Warning Academy, Wuhan 430019, China (e-mail: anlehit@163.com).

Yiping Cui is with the Department of Electronics, Southeast University - Sipailou Campus, Nanjing 210096, China (e-mail: cyp@seu.edu.cn).

Digital Object Identifier 10.1109/JPHOT.2021.3112719

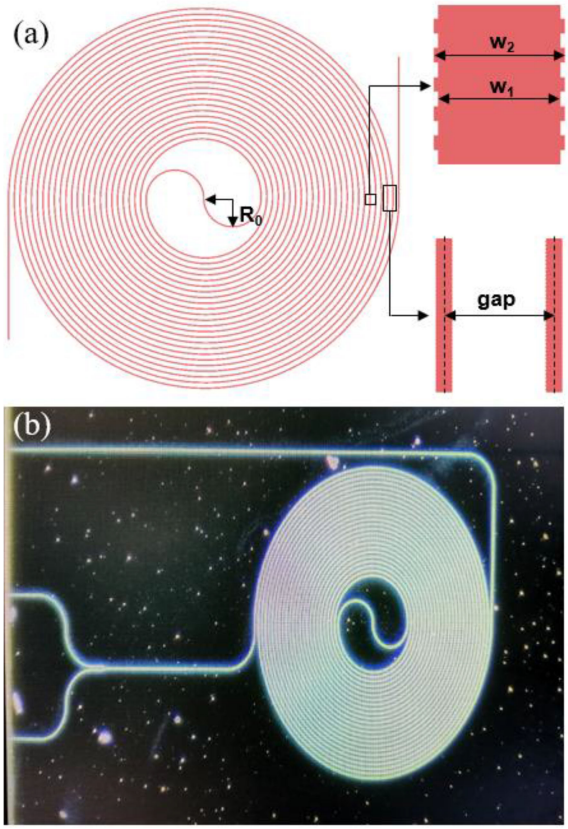

Fig. 1. (a) Schematic of the chirped SBGW. (b) Micrograph of the unapodized chirped SBGW.

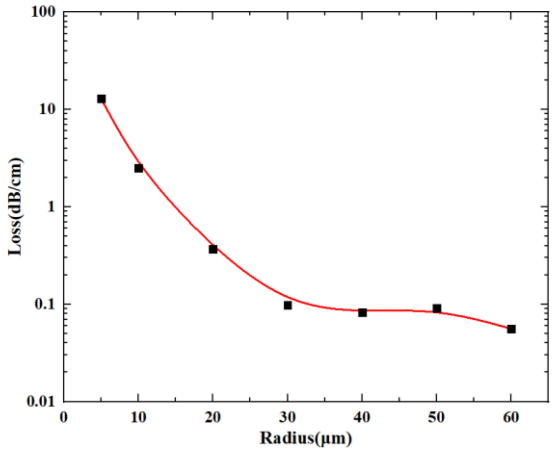

Fig. 2. Calculated bent loss of 1200 nm wide waveguide under different bending radii with fitting curve.

bending radius R_0, waveguides with different bending radii are simulated by FDTD, and the calculated bent losses are shown in Fig. 2. From the calculation results, the value of R_0 is finally set to 40 μm. The corrugation width is chosen to be 40 nm, so that w_1 and w_2 are 1160 nm and 1240 nm, respectively. The center-to-center gap between adjacent waveguides is 8 μm to avoid crosstalk. The maximum radius of the outermost Archimedean spiral is 272 μm, so the overall size of the chirped SBGW is confined to only 0.3 mm^2.

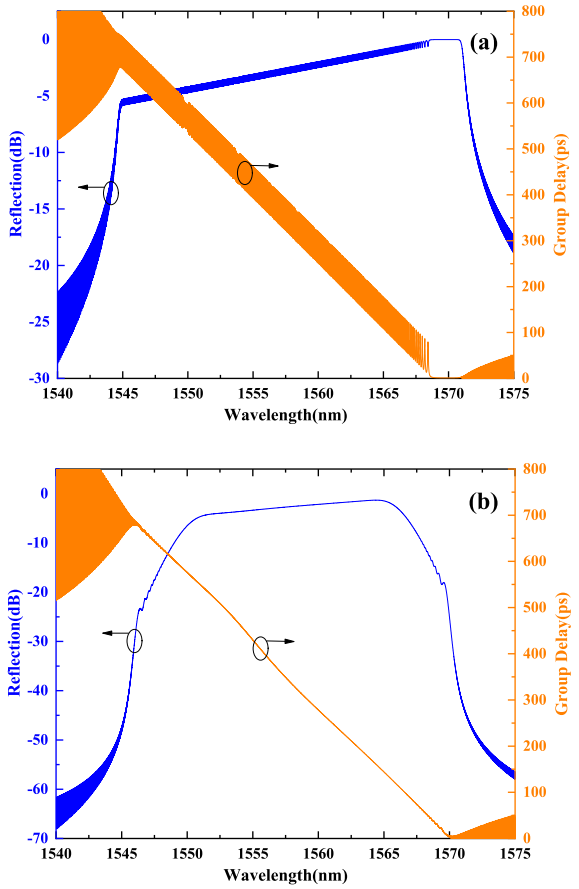

Fig. 3. Simulated reflection spectrum and group delay of (a) unapodized and (b) apodized chirped SBGW.

According to the Bragg Condition

$$\lambda = 2n_{eff}\Lambda \tag{1}$$

the reflection wavelength λ is affected by both n_{eff} and Λ, where n_{eff} is the waveguide effective refractive index and Λ is the period of the SBGW. Since the n_{eff} perturbation caused by the bending radius variation is calculated to be less than 10^{-3} level, the reflection wavelength can be seen only impacted by Λ. In our design, the period varies linearly along the whole length of the SBGW with a total chirp of -6 nm starting from 282 nm.

Simulations are conducted by the transfer-matrix method (TMM). The reflection spectrum of our proposed chirped SBGW is calculated. Defining φ as the phase of the reflection spectrum, from the formula given as follows [29]

$$\tau = \frac{\mathrm{d}\varphi}{\mathrm{d}\omega} = -\frac{\lambda^2}{2\pi c}\frac{\mathrm{d}\varphi}{\mathrm{d}\lambda} \tag{2}$$

the group delay τ can also be extracted by taking the derivative of φ to the angular frequency ω, where c refers to the light speed in vacuum. The propagation loss in the simulations is originally set to 1 dB/cm. The simulation results are given in Fig. 3(a). A total group delay of 660 ps, with a slope of -28 ps/nm over the passband is achieved. The ripples are related to the strength of the index perturbation and can be reduced by decreasing the corrugation width. However, a too small corrugation width may

exceed the limit of contemporary nano-fabrication technology. Another method to suppress the ripples is apodization. In our design, the corrugation widths of the chirped SBGW are modulated by the following Gaussian apodization function:

$$\Delta w = \Delta w_0 e^{-2[\alpha(x-L/2)/2]^2} \tag{3}$$

where Δw_0 is the corrugation width before apodization, and L is the total length of the chirped SBGW. It can be seen that the corrugation width Δw varies along its longitudinal position x. The parameter α is related to the shape of the Gaussian function, and we set it to 3 here. The simulation results of the apodized chirped SBGW are shown in Fig. 3(b). An ideal group delay curve with evidently reduced ripples is demonstrated.

III. Experimental Results

Our SBGWs were fabricated using electron-beam lithography at Applied Nanotools Inc.. A single etch process was performed on an 8.78 mm × 8.78 mm SOI wafer with 220 nm thick top silicon. A 2 μm thick silicon dioxide layer was deposited as the upper cladding. The edges of the wafer were polished for edge coupling by a deep etch process. To minimize the coupling loss, the mode overlap was pre-calculated to match the MFD 4.0 fiber array in our laboratory, and an optimized coupling width of 164 nm was achieved. The coupling waveguide was tapered to 500 nm width within 60 μm from the edge, and further transited to the 1200 nm width multi-mode waveguide by a 200 μm length taper after the Y-branch. The micrograph of the unapodized chirped SBGW is shown in Fig. 1(b).

We first measured the transmission spectra of a 2.7 cm long spiral waveguide with 1200 nm × 220 nm cross section and a 3.2 cm long spiral waveguide with 500 nm × 220 nm cross section. During the fabrication process, sidewall roughness is inevitable, especially for curved waveguides. The waveguide width can be seen randomly modulated by the rough sidewall, so that Fabry-Perot resonance may occur at certain wavelengths [25]. Since the fundamental mode field of the multi-mode waveguide is confined in the center, while that of the single-mode waveguide is expanded to the waveguide edge, the sensitivity to sidewall roughness of the multi-mode waveguide is much less than the single-mode waveguide, which means the Fabry-Perot effect and scattering caused by sidewall roughness are correspondingly much smaller. Therefore, comparing with the transmission characteristics of the 500 nm wide single-mode spiral waveguide, an expected smoother transmission spectrum with obviously lower propagation loss for the 1200 nm wide multi-mode spiral waveguide as shown in Fig. 4 is achieved. The coupling loss for both waveguides is about 10 dB, 3 dB larger than expected due to slight edge abrasion. The propagation loss of the bent multi-mode waveguide is only 0.7 dB/cm, much smaller than 3.8 dB/cm for the bent single-mode waveguide.

The experiment setup for the group delay testing is illustrated in Fig. 5. A single wavelength optical signal is generated by a tunable laser source. A radio frequency signal from the vector network analyzer is then modulated to the optical signal by a phase modulator. The lower sideband is filtered by a tunable band-pass filter for single sideband operation. The optical signal

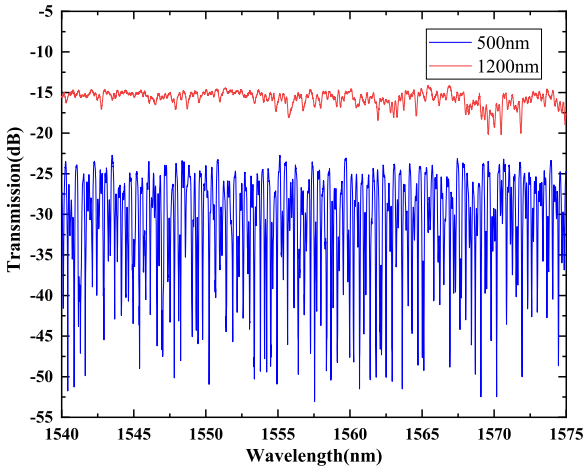

Fig. 4. Measured transmission spectra of 1200 nm wide spiral waveguide of 2.7 cm length and 500 nm wide spiral waveguide of 3.2 cm length.

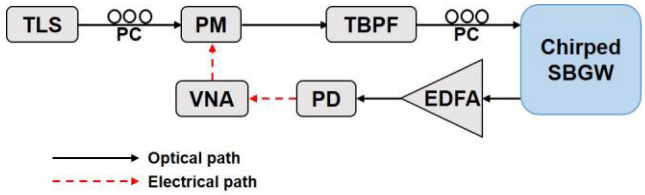

Fig. 5. Experiment setup for the group delay measurement. TLS: tunable laser source; PC: polarization controller; PM: phase modulator; TBPF: tunable band-pass filter; EDFA: Erbium-doped fiber amplifier; PD: photodetector; VNA: vector network analyzer.

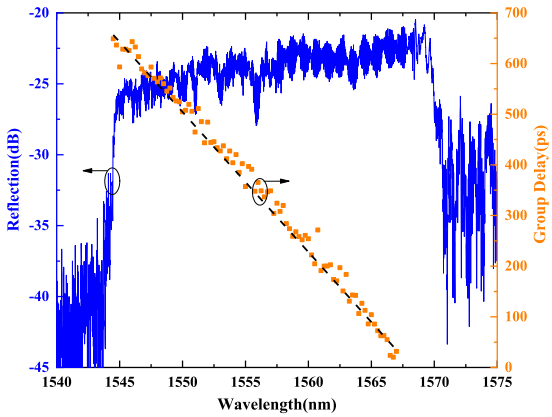

Fig. 6. Measured reflection spectrum and group delay of the unapodized chirped SBGW.

reflected from the chirped SBGW is amplified by an EDFA before demodulation, and the electrical signal is finally transmitted back to the VNA to calculate the group delay. The measurement was carried out at 0.25 nm wavelength interval. The measured group delays as well as the reflection spectrum of the unapodized chirped SBGW are shown in Fig. 6. The experimental results exhibit a total group delay of 628 ps in the range from 1544.5 nm to 1567 nm, with a slope of -27.7 ps/nm, which match well with the simulation results. The power difference between the

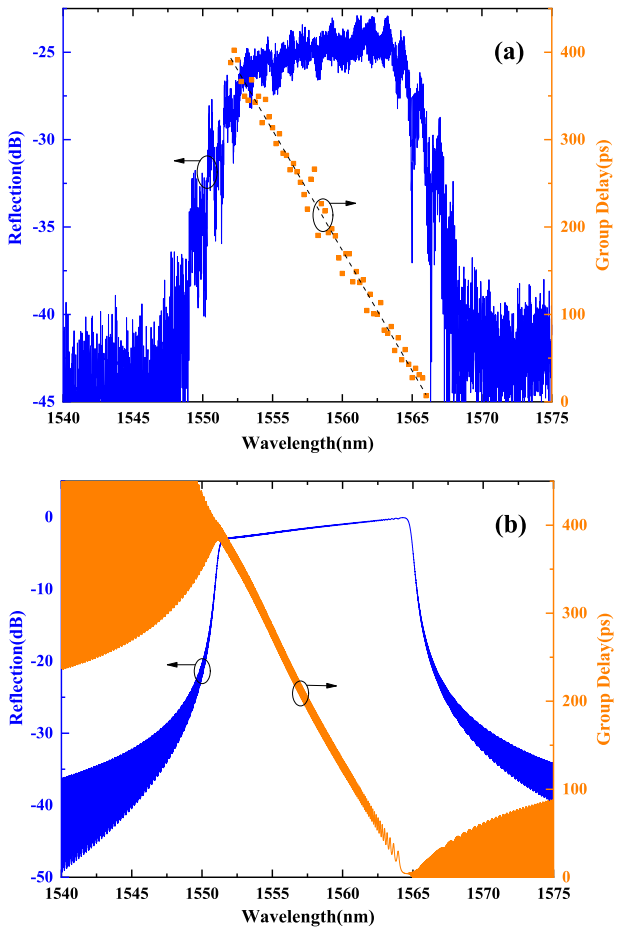

Fig. 7. (a) Measured reflection spectrum and group delay of the apodized chirped SBGW. (b) Simulated reflection spectrum and group delay of the chirped SBGW with apodization width from 10 nm to 40 nm.

minimum and maximum wavelengths is about 3.8 dB, which corresponds to the transmission loss of one round trip in the whole grating, thus a propagation loss of 0.7 dB/cm can be derived. According to the linear fitting of the group delay data points, we can calculate the residual sum of squares (RSS), and an average group delay ripple (AGDR) of ±17.23 ps can be further obtained from the following equation,

$$AGDR = \sqrt{\frac{RSS}{n-1}} \tag{4}$$

where n denotes the number of group delay data points.

The group delays and reflection spectrum of an apodized chirped SBGW were also measured as shown in Fig. 7(a). The average group delay ripple is calculated to be ±12.83 ps, verifying the ripple improvement by applying apodization. However, such experimental results are far from the nearly smooth curve in the simulation results in Fig. 3(b), and the total group delay also decreases. The performance deterioration is attributed to the minimum linewidth limit of nano-fabrication technology. Comparing the passband bandwidths between the apodized and unapodized chirped SBGWs, we applied the bandwidth reduction to the Gaussian apodization function and estimated that the corrugations smaller than 10 nm were failed to be characterized in fabrication. The successfully fabricated sections of the apodized chirped SBGW were further simulated as shown in Fig. 7(b), verifying our explanation of the degraded performance. This result provides a caution for minimum linewidth control in nano-design according to the fabrication technology.

TABLE I
COMPARISON OF SOI CHIRPED BRAGG GRATING WAVEGUIDES

Reference	Waveguide type	Polari -zation	Grating Length	Total group delay
11	220 nm rib	TE	5.76 mm	~140 ps
23	220 nm rib	TE	12.54 mm	241 ps
25	220 nm strip	TM	4 mm	~120 ps
26	220 nm strip	TM	3 mm	31.2 ps
27	1.4 μm rib	TE	2 cm	500 ps
This work	220 nm strip	TE	2.7 cm	628 ps

A comparison of SOI chirped Bragg grating waveguides reported in recent years is listed in Table 1. It can be seen that our SBGW has the longest total length with the largest group delay, showing its application potential in on-chip dispersion. The selection of strip waveguide reduces the demand on minimum bending radius, allowing the usage of compact spiral configuration. Moreover, the standard fabrication technology as well as the TE operation mode makes our design advantageous in integration.

IV. CONCLUSION

In conclusion, a TE mode chirped SBGW on SOI platform with 2.7 cm length and propagation loss as low as 0.7 dB/cm has been fabricated and experimentally demonstrated. A total group delay of 628 ps and a linear dispersion of -27.7 ps/nm are achieved. Benefit from the spiral configuration, the footprint of the structure is only 0.3 mm^2. The group delay ripples are effectively reduced by apodization, and the bandwidth reduction can be avoided by modifying the apodization function according to contemporary nano-fabrication technology. This chirped SBGW shows good compatibility with other optical devices, considering its operation mode, and the low propagation loss characteristic makes it promising in fields relevant to large on-chip dispersion, such as beam-forming and waveform generation.

REFERENCES

[1] T. Ma, K. Nallapan, H. Guerboukha, and M. Skorobogatiy, "Analog signal processing in the terahertz communication links using waveguide Bragg gratings: Example of dispersion compensation," *Opt. Exp.*, vol. 25, no. 10, pp. 11009–11024, May. 2017.

[2] M. M-Dusanowska *et al.*, "Strain-tunable single-photon source based on a circular Bragg grating cavity with embedded quantum dots," *ACS Photon.*, no. 7, pp. 3474–3480, Nov. 2020.

[3] Y. Zhang *et al.*, "Tunable frequency-multiplying optoelectronic oscillator based on a dual-parallel Mach-Zehnder modulator incorporating a phase-shifted fiber Bragg grating," *Optoelectron. Lett.*, vol. 16, no. 6, pp. 0405–0409, Nov. 2020.

[4] O. Krarup *et al.*, "Nonlinear resolution enhancement of an FBG based temperature sensor using the Kerr effect," *Opt. Exp.*, vol. 28, no. 26, pp. 39181–39188, Dec. 2020.

[5] L. Kai, J. Sun, and Y. Gao, "High-resolution detection of wavelength shift induced by an erbium-doped fiber Bragg grating," *J. Lightw. Technol.*, vol. 39, no. 1, pp. 275–281, Jan. 2021.

[6] Y. Liu *et al.*, "Ultrafast optical signal processing with Bragg structures," *Appl. Sci.*, vol. 7, no. 6, pp. 556–571, May. 2017.

[7] M. Burla *et al.*, "Integrated waveguide Bragg gratings for microwave photonics signal processing," *Opt. Exp.*, vol. 21, no. 21, pp. 25120–25147, Oct. 2013.

[8] X. Liang *et al.*, "Spectral-distortionless, flat-top, drop-filter based on complementarily-misaligned multimode-waveguide Bragg gratings," *J. Lightw. Technol.*, vol. 38, no. 23, pp. 6600–6604, Dec. 2020.

[9] A. D. Simard *et al.*, "Bandpass integrated Bragg gratings in silicon-on-insulator with well-controlled amplitude and phase responses," *Opt. Lett.*, vol. 40, no. 5, pp. 736–739, Feb. 2015.

[10] R. Xiao *et al.*, "Integrated Bragg grating filter with reflection light dropped via two mode conversions," *J. Lightw. Technol.*, vol. 37, no. 9, pp. 1946–1953, May. 2019.

[11] Z. Zou *et al.*, "Channel-spacing tunable silicon comb filter using two linearly chirped Bragg gratings," *Opt. Exp.*, vol. 22, no. 16, pp. 19513–19522, Aug. 2014.

[12] J. Jiang *et al.*, "Silicon lateral-apodized add–drop filter for on-chip optical interconnection," *Appl. Opt.*, vol. 56, no. 30, pp. 8425–8429, Oct. 2017.

[13] T. He, J. Demas, and S. Ramachandran, "Ultra-low loss dispersion control with chirped transmissive fiber gratings," *Opt. Lett.*, vol. 42, no. 13, pp. 2531–2534, Jun. 2017.

[14] A. B. Dar and R. K. Jha, "Design and comparative performance analysis of different chirping profiles of tanh apodized fiber Bragg grating and comparison with the dispersion compensation fiber for long-haul transmission system," *J. Mod. Opt.*, vol. 64, no. 6, pp. 555–566, 2017.

[15] M. H. Khan *et al.*, "Ultrabroad-bandwidth arbitrary radiofrequency waveform generation with a silicon photonic chip-based spectral shaper," *Nature Photon.*, vol. 4, pp. 117–122, Feb. 2010.

[16] C. Wang and J. Yao, "Chirped microwave pulse generation based on optical spectral shaping and wavelength-to-time mapping using a Sagnac loop mirror incorporating a chirped fiber Bragg grating," *J. Lightw. Technol.*, vol. 27, no. 16, pp. 3336–3341, Aug. 2009.

[17] X. Zhu, X. Zhu, H. Sun, W. Li, N. Zhu, and M. Li, "Arbitrary waveform generation based on dispersion-free wavelength-to-time mapping technique," *IEEE Photon. J.*, vol. 10, no. 1, Feb. 2018, Art. no. 5500609.

[18] J. Wang, R. Ashrafi, M. Rochette, and L. R. Chen, "Chirped microwave pulse generation using an integrated SiP Bragg grating in a Sagnac loop," *IEEE Photon. Technol. Lett.*, vol. 27, no. 17, pp. 1876–1879, Sep. 2015.

[19] S. Zamek *et al.*, "Compact chip-scale filter based on curved waveguide Bragg gratings," *Opt. Lett.*, vol. 35, no. 20, pp. 3477–3479, Oct. 2010.

[20] A. D. Simard, Y. Painchaud, and S. LaRochelle, "Integrated Bragg gratings in spiral waveguides," *Opt. Exp.*, vol. 21, no. 7, pp. 8953–8963, Apr. 2013.

[21] X. Wang *et al.*, "Precise control of the coupling coefficient through destructive interference in silicon waveguide Bragg gratings," *Opt. Lett.*, vol. 39, no. 19, pp. 5519–5522, Oct. 2014.

[22] X. Wang *et al.*, "Narrow-band waveguide Bragg gratings on SOI wafers with CMOS-compatible fabrication process," *Opt. Exp.*, vol. 20, no. 14, pp. 5547–5558, Jul. 2012.

[23] W. Zhang and J. Yao, "Photonic generation of linearly chirped microwave waveforms using a silicon-based on-chip spectral shaper incorporating two linearly chirped waveguide Bragg gratings," *J. Lightw. Technol.*, vol. 33, no. 24, pp. 5047–5054, Dec. 2015.

[24] W. Zhang and J. Yao, "Silicon-based on-chip electrically-tunable spectral shaper for continuously tunable linearly chirped microwave waveform generation," *J. Lightw. Technol.*, vol. 34, no. 20, pp. 4664–4672, Oct. 2016.

[25] Z. Chen *et al.*, "Spiral Bragg grating waveguides for TM mode silicon photonics," *Opt. Exp.*, vol. 23, no. 19, pp. 25295–25307, Sep. 2015.

[26] M. Ma *et al.*, "Apodized spiral Bragg grating waveguides in silicon-on-insulator," *IEEE Photon. Technol. Lett.*, vol. 30, no. 1, pp. 111–114, Jan. 2018.

[27] I. Giuntoni *et al.*, "Continuously tunable delay line based on SOI tapered Bragg gratings," *Opt. Exp.*, vol. 20, no. 10, pp. 11241–11246, May 2012.

[28] A. D. Simard, A. D. Simard, N. Belhadj, Y. Painchaud, and S. LaRochelle, "Apodized silicon-on-insulator Bragg gratings," *IEEE Photon. Technol. Lett.*, vol. 24, no. 12, pp. 1033–1035, Jun. 2012.

[29] F. Ouellette, "Dispersion cancellation using linearly chirped Bragg grating filters in optical waveguides," *Opt. Lett.*, vol. 12, no. 10, pp. 847–849, Oct. 1987.